ChemPubSoc Europe
DOI: 10.1002/chem.201500737
CHEMISTRY A European Journal
Full Paper

Titanium Complexes | *Hot Paper* |

Ansa-Bridged Bis(benzene) Titanium Complexes

Holger Braunschweig,* Charlotte Brückner, Mehmet Ali Celik, Klaus Dück, Florian Hupp, Thomas Kramer, Johannes Krebs, and Ivo Krummenacher[a]

Abstract: Taking advantage of an improved synthesis of [Ti(η^6-C_6H_6)$_2$], we report here the first examples of *ansa*-bridged bis(benzene) titanium complexes. Deprotonation of [Ti(η^6-C_6H_6)$_2$] with *n*BuLi in the presence of *N*,*N*,*N*′,*N*′′,*N*′′-pentamethyldiethylenetriamine (pmdta) leads to the corresponding 1,1′-dilithio salt [Ti(η^6-C_6H_5Li)$_2$]·pmdta that enables the preparation of the first one- and two-atom-bridged complexes by simple salt metathesis. The *ansa* complexes were fully characterized (NMR spectroscopy, UV/Vis spectroscopy, elemental analysis, and X-ray crystallography) and further studied electrochemically and computationally. Moreover, [Ti(η^6-C_6H_6)$_2$] is found to react with the Lewis base 1,3-dimethylimidazole-2-ylidene (IMe) to give the bent sandwich complex [Ti(η^6-C_6H_6)$_2$(IMe)].

Introduction

Just four years after Kealy, Pauson, Miller, Tebboth, and Tremaine published their landmark discoveries on ferrocene,[1] the first bis(benzene) metal compound was isolated.[2] Although ferrocene became an important organometallic reagent with many applications in organic synthesis and material sciences due to its high stability, ease of functionalization, and cheap availability,[3] the chemistry of bis(arene) sandwich compounds did not advance so rapidly. Among this class of compounds, the non-iron-containing bis(benzene) derivatives [M(η^6-C_6H_6)$_2$] (M = V, Cr, Mo) are one of the most widely used and studied ones (Figure 1).[4] Common to these complexes is the possibility for functionalization by dilithiation, thereby providing access to *ansa* sandwich compounds in which the two benzene ligands are connected by a short bridge.[5] The first examples for such bridged bis(benzene) metal complexes were published by Elschenbroich et al. who managed to isolate vanado- and chromoarenophanes with a silicon atom in the bridging position.[6] After this seminal report, many investigations have focused on the effect of the *ansa* bridge on the properties of these complexes, which led to the preparation of Group 13 element- (B, Al, Ga), Group 14 element- (Si, Ge, Sn), and transition-metal-bridged (Zr) derivatives of [V(η^6-C_6H_6)$_2$] and [Cr(η^6-C_6H_6)$_2$].[5a,6,7]

In contrast, the formation of *ansa* complexes derived from [Mo(η^6-C_6H_6)$_2$] is a more challenging task. For instance, the reaction of the dilithiated species [Mo(η^6-C_6H_5Li)$_2$]·tmeda (tmeda = *N*,*N*,*N*′,*N*′-tetramethylethylenediamine) with the disilane $Cl_2Si_2Me_4$ leads to a mixture of the target product [Mo(η^6-$C_6H_5SiMe_2$)$_2$], the unbridged sandwich complex, and the paracyclophane [Mo(η^6-$C_6H_5Si_2Me_4$)$_2$]. The generation of the cyclophane side product in this process was attributed to the deprotonation of [Mo(η^6-$C_6H_5SiMe_2$)$_2$] by [Mo(η^6-C_6H_5Li)$_2$]·tmeda.[5d] Nevertheless, the selective introduction of a single *ansa* bridge has been achieved by the group of Müller, who reported the first main group element-bridged (Al, Ga, Si) [1]molybdoarenophanes.[8]

Like their better known bis(cyclopentadienyl) counterparts, strained *ansa* bis(benzene) metal complexes possess many interesting properties and reactivities.[3a,5a,6,7b,e] Among the chemical transformations, which include diboration and disilylation reactions,[7f,9] the ring-opening polymerization (ROP) is one of the most widely studied reactions as it can provide access to functional metallopolymers.[4d,7b,d,g] Given that the macromolecular properties of these polymers depend on both the nature of the metal center and the bridging unit, the synthesis of *ansa*-bridged precursors continues to be an important and topical subject.[4e,7b]

In view of this, the 16-electron complex [Ti(η^6-C_6H_6)$_2$] (**1**), which is isoelectronic to troticene [Ti(η^5-C_5H_5)(η^7-C_7H_7)], has sparked our interest. In spite of displaying interesting properties, such as catalytic or redox activity,[10] no *ansa* derivatives have been reported to date. This is in part due to its difficult synthesis, traditionally involving metal vapor co-condensation techniques that are very demanding in their experimental setup (see Scheme 1).[11] However, the group of Bönnemann achieved a more straightforward, condensed-state synthesis of compound **1** with ordinary laboratory equipment through the reduction of $TiCl_4$ with K[BEt_3H] in benzene solution by using ultrasound (Scheme 2).[12]

Herein, we report an improvement to the synthesis of Bönnemann et al. of bis(benzene) titanium (**1**) and describe its first *ansa*-bridged derivatives.

---

[a] *Prof. Dr. H. Braunschweig, C. Brückner, Dr. M. A. Celik, Dr. K. Dück,*
Dr. F. Hupp, Dr. T. Kramer, J. Krebs, Dr. I. Krummenacher
Institut für Anorganische Chemie
Julius-Maximilians-Universität Würzburg
Am Hubland, 97074 Würzburg (Germany)
Fax: (+49) 931-31-84623
E-mail: h.braunschweig@uni-wuerzburg.de

Supporting information for this article is available on the WWW under http://dx.doi.org/10.1002/chem.201500737.

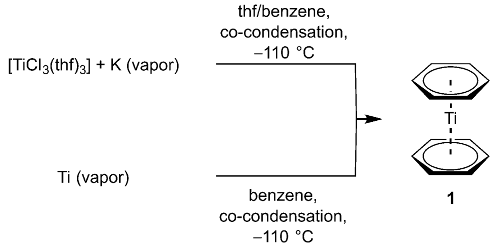

Scheme 1. Preparation methods for bis(benzene) titanium through metal-vapor co-condensation.

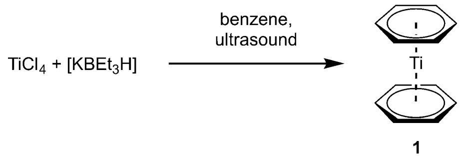

Scheme 2. Preparation of bis(benzene) titanium (**1**) through reduction of $TiCl_4$.

Results and Discussion

Improved synthesis of [Ti(η^6-C_6H_6)$_2$] (1)

For the preparation of bis(benzene) titanium (**1**) we followed the arguably most straightforward route by Bönnemann et al.[12] By using benzene as solvent, instead of a solvent mixture, vigorously stirring the reaction mixture, and maintaining a low temperature during the work-up procedure, we were able to reproducibly improve the yield from the reported 11% to 21%. The use of different reducing agents, such as K, KC_8, or Na, or a change of the reaction conditions (see Table S1 in the Supporting Information for details), however, did not lead to any further improvement in yield.

The composition of compound **1** is supported by NMR spectroscopy (^{1}H NMR: $\delta = 4.92$ ppm, ^{13}C{^{1}H} NMR: $\delta = 79.41$ ppm) and X-ray structure determination. Although the crystal structure of compound **1** has been previously reported in the literature, no structural data is available in the Cambridge Structural Database.[13] This information is thus provided here. Crystals suitable for X-ray structure analysis were grown from a saturated benzene solution at room temperature (Figure S1 in the Supporting Information). The Ti–C bond lengths in the linear sandwich complex range from 224.1(2) to 224.7(2) pm with a Ti–X_{Bz} distance (Bz = benzene, X_{Bz} = centroid of the C_6H_6 or C_6H_5 ring) of 174.8 pm, which is consistent with a parallel arrangement of the benzene ligands (tilt angle $\alpha = 0^\circ$, X_{Bz}-Ti-X_{Bz} (δ) = 180°, for definition of the angles see Figure 6 in the Experimental Section). Related bis(arene) titanium compounds such as bis(toluene) titanium ($\alpha = 2^\circ$, Ti–X_{Bz} 174 pm) or bis(biphenyl) titanium ($\alpha = 0^\circ$, Ti–X_{Bz} 178 pm) show similar structural features.[14]

Reaction of [Ti(η^6-C_6H_6)$_2$] (1) with Lewis bases

The 16-electron configuration of compound **1** suggests that it is able to coordinate ligands to give bent sandwich complexes. Moreover, it is known from isoelectronic complexes, that is, [Ti(η^5-C_5H_5)(η^7-C_7H_7)SiMe$_2$], that it is possible to form CO, isocyanide, and NHC (N-heterocyclic carbene) adducts.[15] We have thus set out to study the reactivity of compound **1** towards neutral Lewis bases. Addition of the N-heterocyclic carbene 1,3-dimethylimidazole-2-ylidene (IMe) to a solution of compound **1** in C_6D_6 led to an instant color change of the solution from deep red to brown (Scheme 3). After recrystallization, adduct **2** was isolated in nearly quantitative yield.

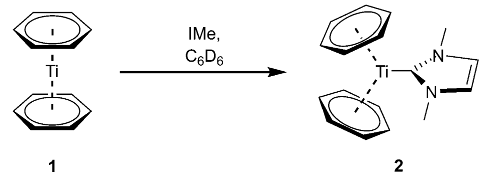

Scheme 3. Reaction of [Ti(η^6-C_6H_6)$_2$] (**1**) with the Lewis base IMe.

The coordination of the carbene is supported by elemental analysis, NMR spectroscopy, and X-ray crystallography. As a result of the adduct formation, the ^{1}H NMR resonances for the benzene ligands show a distinct shift to lower frequencies.[16] It is noteworthy that the ^{13}C NMR resonance for the carbene carbon atom cannot be detected even by using high concentrations or through 2D ^{13}C–^{1}H HSQC and HMBC experiments. Single crystals of compound **2** were grown from a saturated benzene solution at room temperature. Compound **2** crystallizes in the monoclinic space group $P2_1/c$ (Figure 1). Increasing the coordination number on the titanium atom by the two-electron-donating carbene leads to an elongation of the Ti–C_{Bz} distances (227.9(3)–240.2(3) pm, Ti–X_{Bz} 186 pm) compared to the parent compound **1**. The Ti–C(IMe) distance (232.3(3) pm) in compound **2** can be compared with those in a $TiCl_4$–NHC adduct (219.4(7) pm) or adducts derived from the isoelectronic *ansa* complex sila[1]troticenophane.[15e,17] The difference in the bond length between the metal and the carbene is likely related to the different oxidation state of the metal and the coordination environment. The molecule shows a highly bent structure ($\alpha = 37.5(1)$, $\delta = 146.7^\circ$), in which the ring plane of the NHC ligand is perpendicular to the X_{Bz}-Ti-X_{Bz}

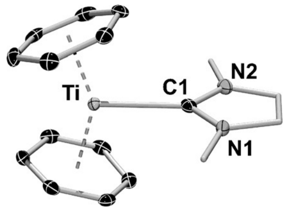

Figure 1. Molecular structure of [Ti(η^6-C_6H_6)$_2$(IMe)] (**2**). Hydrogen atoms are omitted for clarity and only selected displacement ellipsoids, drawn at the 50% probability level, are shown. Selected bond lengths [pm] and angles [°]: Ti–C_{Bz} 227.9(3)–240.2(3), Ti–X_{Bz} 185.4 and 186.5, Ti–C1 232.3(3), $\alpha = 37.5(1)$, $\delta = 146.7$ (X_{Bz} = benzene ring centroid).

axis. Similar structural distortions have been observed for the adducts of trozircene ($\delta = 147.5^\circ$) or trohafcene ($\delta = 147.5^\circ$).[15c,e,f]

Further attempts to induce adduct formation with sterically more demanding NHC ligands (i.e., 1,3-dimesitylimidazol-2-ylidene (IMes), I*t*Bu), other neutral Lewis bases (PR_3, R = methyl, ethyl, or cyclohexyl), or CO were unsuccessful.

Dilithiation of [Ti(η^6-C_6H_6)$_2$] (1)

With compound **1** in hand, we were able to carry out the selective 1,1′-dimetalation of the benzene ligands with 2.5 equivalents of *n*BuLi and *N*,*N*,*N*′,*N*″,*N*″-pentamethyldiethylenetriamine (pmdta, Scheme 4). [Ti(η^6-C_6H_5Li)$_2$]·pmdta (**3**·pmdta) was obtained in 92 % yield as brownish-red solid. The ^1H NMR spectrum recorded in D_8[THF], which causes the displacement of the pmdta molecules by the D_8[THF] molecules, shows two multiplets at $\delta = 4.70$ and 4.92 ppm in a 3:2 ratio for the protons of the benzene rings and signals for the free pmdta molecules in the region $\delta = 2.15$–2.41 ppm, analogous to other dilithiated bis(benzene) metal complexes.[5d] The $^{13}C\{^1H\}$ and $^7Li\{^1H\}$ NMR spectra are also in agreement with the proposed structure. Consistent with the ^1H NMR spectrum, elemental analysis indicates that there is one pmdta molecule associated with one sandwich unit.

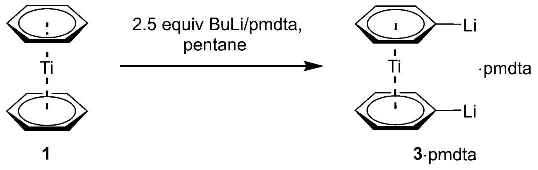

Scheme 4. Selective dilithiation of [Ti(η^6-C_6H_6)$_2$] (**1**).

Synthesis of single- and double-atom-bridged titanoarenophanes

By using compound **3**·pmdta as reagent in salt metathesis reactions with Group 14 element dihalides, a number of different *ansa* bridges could be introduced. Treatment of the dilithiated complex with 1,1,2,2-tetramethyldichlorodisilane or 1,1,2,2-tetra(*tert*-butyl)dichlorodistannane at −78 °C and subsequent warming to room temperature led to the isolation of the two-atom-bridged complexes **4** and **5**, respectively (Scheme 5). After recrystallization, the titanoarenophanes were isolated as deep red solids in moderate yields (36–46 %). The identity of these compounds was unambiguously confirmed by elemental analysis and NMR spectroscopy. The ^1H NMR spectra of the silicon- and tin-bridged titanoarenophanes **4** and **5** display one signal for the equivalent methyl and *tert*-butyl substituents (**4**: $\delta = 0.29$ ppm; **5**: $\delta = 1.49$ ppm, $J(^{119}Sn,^1H_{tBu}) = 66$ Hz, $J(^{117}Sn,^1H_{tBu}) = 63$ Hz) and three multiplets with an intensity ratio of 2:2:1 for the three inequivalent protons of the aromatic benzene rings (**4**: $\delta = 5.14$, 5.21, and 5.40 ppm; **5**: $\delta = 5.06$, 5.18, and 5.53 ppm).

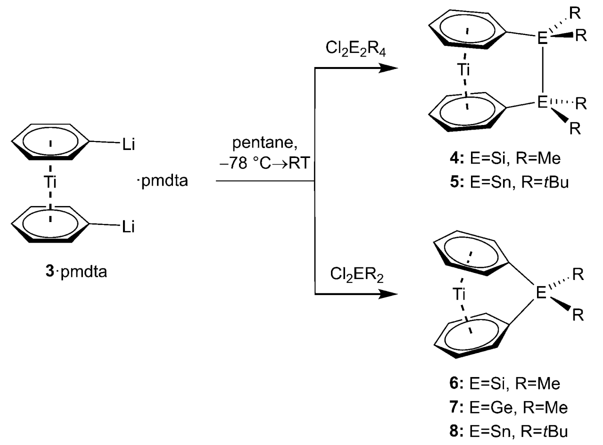

Scheme 5. Conversion of [Ti(η^6-C_6H_5Li)$_2$]·pmdta (**3**·pmdta) to *ansa* sandwich complexes.

In the same manner, we prepared the single-atom-bridged titanoarenophanes (Scheme 5). The salt metathesis of compound **3**·pmdta with Cl_2SiMe_2, Cl_2GeMe_2, or $Cl_2Sn\mathit{t}Bu_2$ resulted in the isolation of the strained *ansa* complexes **6**–**8**. After work-up, the complexes were obtained in satisfactory yields (i.e., **6**: 32 %, **7**: 43 %, **8**: 29 %) as light red to orange solids. The composition of the compounds was confirmed by elemental analysis and NMR spectroscopy. Whereas complexes **6** and **7** show a singlet for the methyl protons in the ^1H NMR spectrum (**6**: $\delta = 0.05$ ppm; **7**: $\delta = 0.15$ ppm), the resonance for the methyl protons in complex **8** display additional tin satellites (**8**: $\delta = 1.33$ ppm, $J(^{119}Sn,^1H_{tBu}) = 71$ Hz, $J(^{117}Sn,^1H_{tBu}) = 68$ Hz). In contrast to the less distorted derivatives **4** and **5**, one multiplet of the ring protons in the single-atom-bridged compounds **6**–**8** is shifted to lower frequencies (**6**: $\delta = 4.07$ ppm; **7**: $\delta = 3.99$ ppm; **8**: $\delta = 4.44$ ppm) compared to compounds **4** and **5**. Similarly, a characteristic shift of the resonances for the ring *ipso*-carbon atoms to lower frequencies can be observed in the $^{13}C\{^1H\}$ NMR spectrum (**4**: $\delta = 87.11$ ppm; **5**: $\delta = 93.74$ ppm vs. **6**: $\delta = 40.41$ ppm; **7**: $\delta = 35.47$ ppm; **8**: $\delta = 46.07$ ppm).

The changes in the NMR chemical shifts are consistent with the presence of a considerable amount of distortion in the [1]titanoarenophanes **6**–**8**, as similar observations were previously noted for *ansa*-ferrocenes and other metalloarenophanes.[6,7,18]

Additionally, the $^{13}C\{^1H\}$ NMR and the heteronuclear NMR spectra (i.e., $^{29}Si\{^1H\}$ or $^{119}Sn\{^1H\}$ NMR) of all compounds are in agreement with the proposed structures. In the heteronuclear NMR spectra of the single-atom-bridged compounds **6** ($^{29}Si\{^1H\}$ NMR: $\delta = 7.38$ ppm) and **8** ($^{119}Sn\{^1H\}$ NMR: $\delta = 2.06$ ppm) the expected downfield shift of the resonances can be observed compared to the two-atom-bridged analogues **4** ($^{29}Si\{^1H\}$ NMR: $\delta = -21.72$ ppm) and **5** ($^{119}Sn\{^1H\}$ NMR: $\delta = -31.20$ ppm), as previously reported for comparable *ansa*-metalloarenes.[6,7f,19]

It is also worth noting that for all complexes weak ^1H NMR signals for the formation of the free flytrap ligand were observed within several hours, indicating some degree of thermal instability in solution. Although no visible color change of the solution can be observed, an insoluble black solid begins to precipitate after a few hours. In the solid state, however, the *ansa* complexes seem to be stable, as no color change can be observed over time and the ^{1}H NMR spectrum does not show any signs of decomposition if acquired shortly after dissolution.

Molecular structures of the [1]- and [2]titanoarenophanes

X-ray crystal structure analyses could be performed on all *ansa* complexes except compound **6**. The crystallographic data for the disila[2]titanoarenophane **4** (Figure 2) indicate that the distances between the metal and the carbon atoms of the benzene ligands are within a narrow range of 223.7(1) to 226.6(1) pm with a Ti–X_{Bz} distance of 174.0 pm (Si1–Si2 234.1(1) pm). The two benzene rings are essentially eclipsed but deviate from a parallel arrangement, as seen by the tilt angle of $\alpha = 7.3°$ and the X_{Bz}-Ti-X_{Bz} angle of $\delta = 174.7°$. The C_{ipso}–Si bond is slightly bent out of the ring plane by $\beta = 10.7°$. Analogous systems with the transition metals vanadium and chromium have comparable structures ([V(η^6-$C_6H_5SiMe_2$)$_2$]: V–C_{Bz} 219.0(2)–220.9(3) pm, V–X_{Bz} 168.1 and 167.6 pm, Si1–Si2 234.22(8) pm, $\alpha = 4.4(2)°$, $\delta = 176.8°$; [Cr(η^6-$C_6H_5SiMe_2$)$_2$]: Cr–C_{Bz} 214.3(2)–216.0(3) pm, Cr–X_{Bz} 161.6 and 162.2 pm, Si1–Si2 233.94(8) pm, $\alpha = 2.8(2)°$, $\delta = 177.8°$).[5a,6,7]

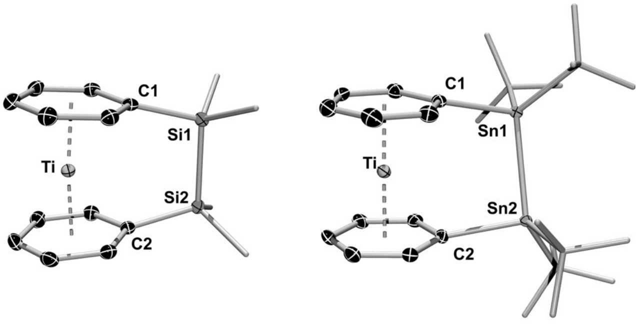

4

5

Figure 2. Molecular structure of [Ti(η^6-$C_6H_5SiMe_2$)$_2$] (**4**, left) and [Ti(η^6-$C_6H_5SntBu_2$)$_2$] (**5**, right). Only one of the two independent molecules in the unit cell of compound **5** is shown and discussed. Symmetry elements in the structure of compound **4**: *x*, $-y+1/2$, *z*. Hydrogen atoms and thermal ellipsoids of the substituents at the bridging atoms are omitted for clarity. Thermal ellipsoids are displayed at the 60 (**4**) and 50% (**5**) probability levels. Selected bond lengths [pm] and angles [°]: **4**: Ti–C_{Bz} 223.7(1)–226.6(1), Ti–X_{Bz} 174.0, Si1–Si2 234.1(1), $\alpha = 7.3(1)$, $\beta = 10.7$, $\gamma = 0$, $\delta = 174.7$, C1-Si1-Si2 104.5(1), C2-Si2-Si1 104.2(5); **5**: Ti–C_{Bz} 223.4(4)–227.0(4), Ti–X_{Bz} 174.1 and 175.0, Sn1–Sn2 282.9(1), $\alpha = 2.6(3)$, $\beta = 9.6$ and 11.3, $\gamma = 22.8$, $\delta = 178.7$, C1-Sn1-Sn2 95.6(2), C2-Sn2-Sn1 96.8(1).

As the crystallographic analysis of the sandwich compound **5** with a [Sn_2tBu_4] bridge (Figure 2) revealed two independent molecules in the asymmetric unit with almost identical structural parameters, only one of the molecular structures will be discussed. The incorporation of a distannane bridge leads to only little distortion of the [Ti(η^6-C_6H_5)$_2$] unit, as illustrated by the angles $\alpha = 2.6(3)$, $\delta = 178.7$, and $\beta_{Bz} = 9.6/11.3°$. The metal–carbon distances also only vary slightly (223.4(4)–227.0(4) pm) and the Ti–X_{Bz} distance ($\approx$174.6 pm) is almost unchanged compared to that of the parent compound **4** (174.7 pm).[13] However, the *ansa* bridge introduces a significant twist in the eclipsed conformation of the benzene rings (C_{ipso}-X_{Bz}-X_{Bz}-C_{ipso} (γ) = 22.8°). The structural parameters can be compared to that of the isoelectronic complex [Ti(η^5-$C_5H_4SntBu_2$)(η^7-$C_7H_6SntBu_2$)], which possesses similar tilt and torsion angles (Sn1-Sn2 283.22(5) pm, $\alpha = 2.0$, $\beta_{Cp} = 6.3$, $\beta_{Cht} = 18.7$, $\gamma = 30.6(2)$ and $\delta = 178.5°$; Cp = C_5H_4 ring, Cht = C_7H_6 ring).[19]

Although we could confirm the connectivity of the single-atom-bridged complex **6** by single-crystal X-ray diffraction, the quality of the data did not allow a detailed discussion of its metric parameters. However, we were able to obtain high-quality diffraction data for the related [1]titanoarenophanes **7** and **8**.

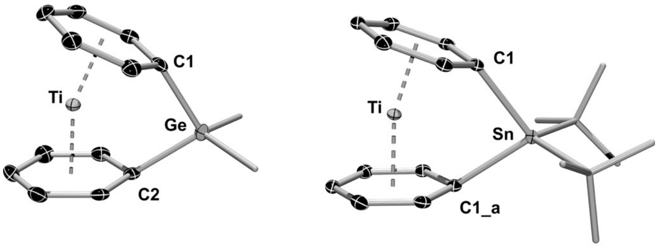

7

8

Figure 3. Molecular structure of [Ti(η^6-C_6H_5)$_2$GeMe$_2$] (**7**, left) and [Ti(η^6-C_6H_5)$_2$SntBu$_2$] (**8**, right). Only one of the three independent molecules in the unit cell of compound **7** is shown and discussed. Symmetry-related positions in the structure of compound **8** ($-x+2$, *y*, $-z+3/2$) are labeled with "_a". Hydrogen atoms and thermal ellipsoids of the substituents at the bridging atoms are omitted for clarity. Thermal ellipsoids are displayed at the 50% probability level. Selected bond lengths [pm] and angles [°]: **7**: Ti–C_{Bz} 221.8(3)–229.4(3), Ti–X_{Bz} 174.1 and 174.4, $\alpha = 25.2(2)$, $\beta = 33.0$, and 33.2, $\delta = 159.1$, $\theta = 91.4(2)$; **8**: Ti–C_{Bz} 219.6(3)–226.8(4), Ti–X_{Bz} 173.3, $\alpha = 19.9(1)$, $\beta = 33.0$, $\delta = 164.1$, $\theta = 86.3(2)$.

The X-ray structural analysis of compound **7** (Figure 3) shows three independent molecules in the unit cell with similar geometrical parameters. Furthermore, the rings are considerably tilted ($\alpha = 25.2(2)$, $\delta = 159.1°$) and the bridging atom is well removed from the plane formed by the benzene ligands ($\beta_{Bz} \approx 33.1°$). The two Ge–C_{ipso} bonds form an angle of $\theta = 91.4(2)°$, a clear deviation from the ideal bond angle of a sp^3-hybridized germanium atom. The Ti–C bond lengths, which extend over the wide range 221.8(3) to 229.4(3) pm (Ti–X_{Bz} = 174.3 pm) further illustrate the distorted geometry and significant strain in the molecule. The geometrical parameters of compound **7** are very similar to those of the isoelectronic complex [Ti(η^5-C_5H_4)(η^7-C_7H_6)GeMe$_2$] ($\alpha = 22.9$, $\beta_{Cp} = 28.5$, $\beta_{Cht} = 28.5$, $\delta = 161.0$, $\theta = 92.8°$).[15d] On the other hand, the ring strain is much more pronounced in compound **7** than the analogous chromium complex [Cr(η^6-C_6H_5)$_2$GeMe$_2$] ($\alpha = 14.4(2)°$).[7e]

X-ray analysis of the crystal structure of compound **8** verifies the successful incorporation of a single tin atom between the two benzene rings (Figure 3). Both rings are significantly displaced from a parallel arrangement ($\alpha = 19.9(1)$, $\delta = 164.1°$) and the C_{ipso}–Sn bond is bent out of the ring plane by $\beta_{Bz} = 33.0°$. Furthermore, the bond angle at the Sn atom deviates substantially from sp^3 hybridization (e.g., C1-Sn-C1_a (θ) =

86.3(1)°). In agreement with these geometrical changes are the variations in the Ti–C distances, which range from 219.6(3) to 226.8(4) pm. Compared to compound **7**, the molecular distortion is less pronounced due to the larger atom in the bridging position.[20] Its molecular strain can be compared to the isoelectronic complex [Ti(η^5-C_5H_4)(η^7-C_7H_6)SnMes$_2$], which shows an interplanar ring angle of $\alpha = 17.2°$ and a X_{Bz}-Ti-X_{Bz} (δ) angle of 165.7°.[19] The related complex [V(η^6-C_6H_5)$_2$Sn*t*Bu$_2$] shows smaller geometrical changes ($\alpha = 15.6$, $\delta = 168.0°$), as a result of the smaller atomic radius of the central metal.[21]

By comparison of all molecular structures, it can be concluded that compound **7** possesses the greatest degree of distortion (Table 1).

Table 1. Structural parameters of the presented bis(benzene) titanoarenophanes. For an explanation of the parameters that define the geometry of the complexes, see Figure 6.

	4	**5**	**7**	**8**
α [°]	7.3(1)	2.6(3)	25.2(2)	19.9(1)
β [°]	10.7	9.6, 11.3	33.1	Bz: 33.0
δ [°]	174.7	178.7	159.1	164.1
θ [°]	104.5(1), 104.2(5)	95.6(2), 96.8(1)	91.4(2)	86.3(1)
γ [°]	0.0	22.8	–[a]	–[a]

[a] No data available.

UV/Vis spectroscopy

To investigate the electronic structure of the presented *ansa* complexes derived from [Ti(η^6-C_6H_6)$_2$] (**1**) we performed solution UV/Vis spectroscopic studies in benzene (for compound **2**) or *n*-hexane in a wavelength region of $\lambda = 220$ to 900 nm (Figures S2–S6 in the Supporting Information). The UV/Vis spectrum of the parent compound [Ti(η^6-C_6H_6)$_2$] (**1**) shows a weak absorption at $\lambda = 233$ nm with a shoulder at $\lambda = 285$ nm. In addition, it shows a global maximum at $\lambda = 345$ nm and a lowest-energy absorption band at $\lambda = 500$ nm (Figure S2 in the Supporting Information). The coordination of the carbene IMe in the bent sandwich complex **2** ($\lambda_{max} = 356$ nm, $\lambda = 497$ nm, Figure S3 in the Supporting Information) does not notably affect the energies or shape of the UV/Vis absorption bands compared to compound **1**.

Linkage of the two benzene rings with a two-atom *ansa* bridge leads to a slight distortion of the structure and thus a bathochromic shift of the lowest-energy band (**4**: $\lambda =$ 529 nm; **5**: $\lambda = 522$ nm, Figure S4 in the Supporting Information). However, this trend is reversed for the more bent molecules **6**–**8** which show blue-shifted transitions (**6**: $\lambda_{max} =$ 460 nm; **7**: $\lambda_{max} = 463$ nm; **8**: $\lambda_{max} = 458$ nm, Figures S4–S6 in the Supporting Information, Table 2) compared to compound **1**. Thus, no general correlation between the tilt angle α and the lowest-energy band absorptions can be established for this series of [1]- and [2]titanoarenophanes. Likewise, the *ansa* complexes derived from [V(η^6-C_6H_6)$_2$] and [Cr(η^5-C_5H_5)(η^6-C_6H_6)] show no correlation between α and λ_{max}.[4e,21,22]

Table 2. Correlation between λ_{max} and the tilt angle α.

	λ_{max} [nm]	α [°]
1	500	0.0(1)
2	497	−37.5(1)
4	529	7.3(1)
5	522	2.6(3)
6	460	–[a]
7	463	25.2(2)
8	458	19.9(1)

[a] Not available.

DFT calculations

DFT calculations were carried out to analyze the character and the energies of the frontier molecular orbitals of the unbridged (i.e., compound **1**), the one- (i.e., compound **4**), and the two-atom-bridged (i.e., compound **6**) complexes. The optimized geometries of compounds **1** and **4** at the B3LYP/def2-SVP level are in good agreement with the experimental ones (see Figures S7 and S8 in the Supporting Information). For the unbridged system [Ti(η^6-C_6H_6)$_2$] (**1**) two approximately isoenergetic highest occupied molecular orbitals (HOMOs) can be found (HOMO and HOMO−1), which are split by introduction of an *ansa* bridge (Figure 4). The HOMO is a bonding combination of titanium d orbitals (d_{xy} and $d_{x^2-y^2}$) with ligand p orbitals, whereas the lowest unoccupied molecular orbital (LUMO) is essentially d_{z^2} in character. The DFT results further suggest that the HOMO–LUMO gap slightly increases for compound **4** ($\Delta E =$ 2.748 eV) with a two-atom bridge, and significantly for the more bent compound **6** ($\Delta E = 2.813$ eV) in comparison to the unbridged complex **1** ($\Delta E = 2.728$ eV). This is, at least in part, consistent with the observed blue shift of the maximum UV/Vis absorption of compound **6** ($\lambda_{max} = 460$ nm) compared to complex **1** ($\lambda_{max} = 500$ nm). It is interesting to note that the predicted change in the band gap of compound **4** is almost negligible despite the moderate torsion of the rings from the coplanar arrangement (see above). In fact, the UV/Vis absorption band for compound **4** ($\lambda_{max} = 529$ nm) suggests a smaller band gap than complex **1** ($\lambda_{max} = 500$ nm).[5a,15a,e]

Cyclic voltammetry

Given the electron-rich nature and the reported reduction chemistry of bis(arene) titanium(0) complexes,[10a] we investigated the redox behavior of all compounds by cyclic voltammetry (Figure 5 and Figures S10–S15 in the Supporting Information). The *ansa* complexes display a chemically irreversible (compounds **4**–**6**, and **8**) or a partially chemically reversible (compound **7**) reduction event at around $E_{pc} = -2.90$ V, which is slightly shifted to more positive values compared to the unbridged species **1** [$E_{1/2} = -2.95$ V vs. ferrocene/ferrocenium (Fc/Fc$^+$)]. The reduction process likely corresponds to the formation of the respective monoanionic complexes, for which, in the case of unbridged bis(arene) titanium complexes, examples have been described.[15f] In addition, the *ansa*-bridged compounds exhibit a chemically irreversible oxidation wave in the

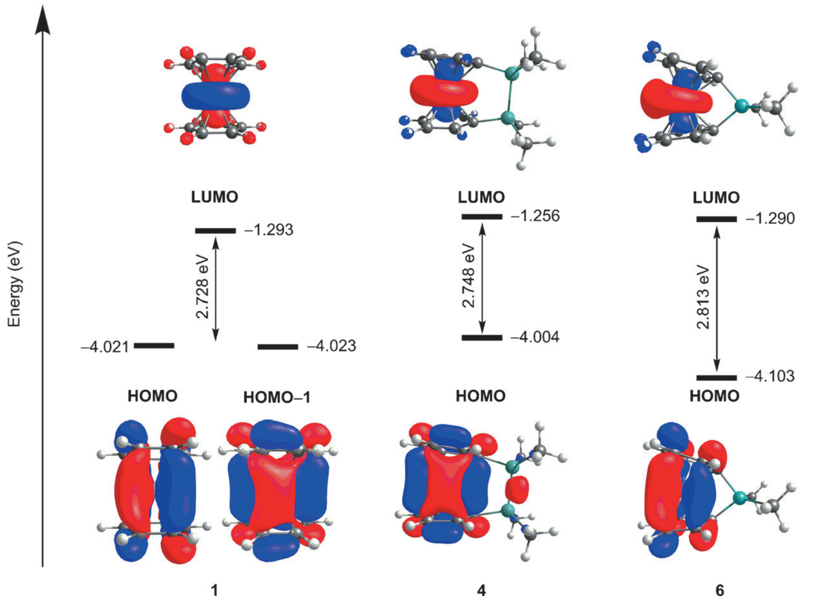

Figure 4. Representation of the frontier orbitals of complexes **1**, **4**, and **6** with their corresponding energy gaps.

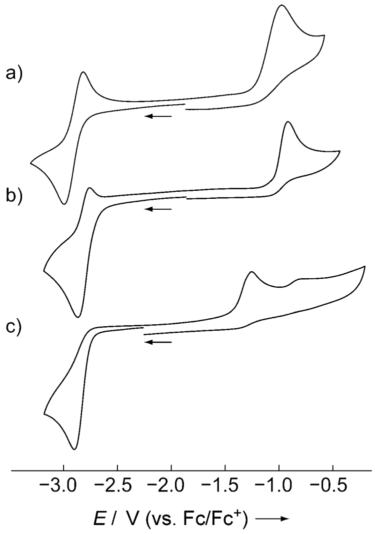

Figure 5. Cyclic voltammograms of compounds a) **1**, b) **4**, and c) **6** in THF/0.1 M [nBu$_4$N][PF$_6$] (scan rate = 250 mV s^{-1}).

range of $E_{pa}=-0.95$ to -1.25 V, comparable to compound **1** ($E_{pa}=-1.10$ V). The irreversible oxidation process presumably involves the loss of a benzene ligand, as can be expected from removal of electrons from the HOMO, which contains metal–ligand bonding interactions.

Conclusion

In summary, we have developed a route to unprecedented *ansa*-bridged bis(benzene) titanium complexes through dilithiation of the bis(arene) precursor and subsequent salt metathesis with Group 14 element halides. As shown by X-ray diffraction analysis, incorporation of the two-atom bridges [Si$_2$Me$_4$] and [Sn$_2$$tBu_4$] introduces only a small amount of molecular distortion, whereas the single-atom bridges [SiMe$_2$], [GeMe$_2$], and [SntBu$_2$] lead to major structural distortions. Despite the electron-rich nature of these complexes, electrochemical characterization indicates that they are susceptible to reduction reactions. Furthermore, bis(benzene) titanium was found to react with an N-heterocyclic carbene to give the corresponding bent sandwich complex [Ti(η^6-C$_6$H$_6$)$_2$(L)] (L = IMe). It is hoped that the more ready availability of bis(benzene) titanium will provide an impetus for further exploration.

Experimental Section

General considerations: All manipulations were performed either under an atmosphere of dry argon or in vacuum by using standard Schlenk line or glovebox techniques. Solvents were dried according to standard procedures, freshly distilled before use, degassed, and stored under argon over molecular sieves (4 Å). 1,3-Dimethylimidazole-2-ylidene (IMe),[16,23] Cl$_2$Sn$_2$$tBu_4$,[24] and Cl$_2SntBu_2$[24] were prepared according to literature procedures. TiCl$_4$ (Merck Chemicals) was distilled under an atmosphere of dry argon and stored under argon. K[BEt$_3$H] was freshly prepared according to a known literature protocol in benzene and directly used for the reduction.[25] nBuLi was purchased from Aldrich as 1.6 mol L^{-1} solution in hexane. *N*,*N*,*N*′,*N*′′,*N*′′-pentamethyldiethylenetriamine (pmdta) was obtained from ABCR, dried over potassium, and distilled under argon before use. Cl$_2$Si$_2$Me$_4$, Cl$_2$SiMe$_2$, and Cl$_2$GeMe$_2$ were obtained from ABCR and used without further purification.

A Bandelin Sonorex RK 100 ultrasonic bath (system voltage: U = 230 V ≈ 50–60 Hz, power input: I = 0.4 A, rated HF-power: P = 80/320 W, HF frequency: f = 35 kHz) was used for ultrasound irradiation. NMR spectra in solution were acquired on a Bruker Avance 500 spectrometer (^{1}H: 500.1 MHz, ^{7}Li{^{1}H}: 194.4 MHz, ^{13}C{^{1}H}: 125.8 MHz, ^{29}Si{^{1}H}: 99.4 MHz, ^{119}Sn{^{1}H}: 186.5 MHz). ^{1}H, ^{13}C{^{1}H}, and ^{29}Si{^{1}H} NMR spectra were referenced to external TMS through the residual protons of the solvent (^{1}H) or the solvent itself (^{13}C). ^{7}Li{^{1}H} NMR spectra were referenced to external LiCl. ^{119}Sn{^{1}H} NMR spectra were referenced to Me$_4$Sn. All chemical shifts are presented in ppm. Elemental analysis was performed on a Leco CHNS-932 Elemental Analyzer. UV/Vis spectra were recorded on a JASCO V-660 UV/Vis spectrometer. Cyclic voltammetry experiments were performed by using a Gamry Instruments Reference 600 potentiostat. A standard three-electrode cell configuration was employed by using a gold disk working electrode, a platinum wire counter electrode, and a silver wire, separated by a Vycor tip, serving as the reference electrode. Formal redox potentials are referenced to the ferrocene/ferrocenium redox couple ([Cp$_2$Fe]$^{+/0}$). Tetra-*n*-butylammonium hexafluorophosphate ([nBu$_4$N][PF$_6$]) was employed as the supporting electrolyte. Compensation for resistive losses (*i*R drop) was employed for all measurements.

Improved synthesis of [Ti(η^6-C$_6$H$_6$)$_2$] (1): To a well-stirred yellow solution of TiCl$_4$ (2.34 mL, 4.04 g, 21.3 mmol) in benzene (50 mL) was added a freshly prepared solution of K[BEt$_3$H] (11.77 g, 85.2 mmol) in benzene (200 mL) over a period of 1 h during ultrasound treatment. The deep red to black reaction mixture was stirred for another hour and the ultrasonic bath was removed. The dark red solution was carefully separated from all precipitates through filtration through a broad Celite pad and subsequently all volatiles were removed in vacuum. The reddish brown residue was washed with a small amount of hexane (5 mL) at −78 °C, dissolved in benzene, and the insoluble precipitate was filtered off. After removal of the solvent under vacuum, compound **1** was isolated as a deep red solid. Additionally, compound **1** can be obtained as deep red to black crystals from a concentrated hexane solution after storing at −70 °C for one day. The combined solids gave $[Ti(\eta^6\text{-}C_6H_6)_2]$ (**1**) as reddish-brown solid (912 mg, 4.47 mmol, 21 %). ^1H NMR (C_6D_6, 500.1 MHz): $\delta = 4.92$ ppm (s, 12H; CH); $^{13}C\{^1H\}$ NMR (C_6D_6, 125.8 MHz): $\delta = 79.41$ ppm (CH); UV/Vis (**5**) (hexane): λ_{max} (ε) = 233 (3724), 285 (sh), 345 (20 561), 500 nm (248 L mol^{-1} cm^{-1}).

$[Ti(\eta^6\text{-}C_6H_6)_2(IMe)]$ (2): To a solution of $[Ti(\eta^6\text{-}C_6H_6)_2]$ (**1**) (20 mg, 98 μmol) in C_6D_6 (0.3 mL) a solution of IMe (10 mg, 98 μmol) in C_6D_6 (2 mL) was added. An immediate color change from deep red to brown was observed. After filtration and recrystallization from a saturated benzene solution, $[Ti(\eta^6\text{-}C_6H_6)_2(IMe)]$ (**2**) was obtained as black crystals (29 mg, 97 μmol, 98 %). ^1H NMR (500.1 MHz, C_6D_6): $\delta = 3.42$ (s, 6H; NCH_3), 4.75 (s, 12H; $CH^{benzene}$), 6.18 ppm (s, 2H; CH^{NHC}); $^{13}C\{^1H\}$ NMR (125.8 MHz, C_6D_6): $\delta = 37.89$ (NCH_3), 79.33 ($C^{benzene}H$), 119.50 ppm ($C^{NHC}H$); UV/Vis (benzene): λ_{max} (ε) = 356 (37 517), 497 nm (415 L mol^{-1} cm^{-1}); elemental analysis calcd (%) for $C_{17}H_{20}N_2Ti$ (304.00): C 67.97, H 6.72, N 9.33; found: C 66.39, H 6.53, N 9.47.

Synthesis of $[Ti(\eta^6\text{-}C_6H_5Li)_2]\cdot pmdta$ (3·pmdta): A suspension of $[Ti(\eta^6\text{-}C_6H_6)_2]$ (**1**) (340 mg, 1.67 mmol) in pentane (15 mL) was treated with BuLi (2.60 mL, 4.16 mmol) and pmdta (721 mg, 4.16 mmol) at room temperature and heated to 40 °C over a period of 12 h. The resulting brown precipitate was collected by filtration, washed with pentane (3×10 mL), and subsequently dried in vacuum to afford $[Ti(\eta^6\text{-}C_6H_5Li)_2]\cdot pmdta$ (**3**·pmdta) as a brown powder (600 mg, 1.54 mmol, 92 %). ^1H NMR (D_8[THF], 500.1 MHz): $\delta = 2.14$ (s, 24H; $N(CH_3^{pmdta})$), 2.20 (s, 6H; $N(CH_3^{pmdta})$), 2.31 (t, 8H; CH_2^{pmdta}), 2.41 (t, 8H; CH_2^{pmdta}), 4.67–4.73 (m, 6H; $CH^{benzene}$), 4.89–4.93 ppm (m, 4H; $CH^{benzene}$); $^{13}C\{^1H\}$ NMR (D_8[THF], 125.8 MHz): $\delta = 43.71$ ($N(C^{pmdta}H_3)$), 46.18 ($N(C^{pmdta}H_3)_2$), 56.67 ($C^{pmdta}H_2$), 58.68 ($C^{pmdta}H_2$), 76.67 ($C^{benzene}H$), 77.59 ($C^{benzene}H$), 87.91 ($C^{benzene}H$), 123.30 ppm ($C^{benzene}$); ^7Li NMR (D_8[THF], 194.4 MHz): $\delta = 2.26$ ppm; elemental analysis calcd (%) for $C_{21}H_{33}Li_2N_3Ti$ (389.25): C 64.74, H 8.54, N 10.79; found: C 64.72, H 8.94, N 10.42.

Synthesis of $[Ti(\eta^6\text{-}C_6H_5SiMe_2)_2]$ (4): A slurry of compound **3**·pmdta (250 mg, 0.64 mmol) in pentane (10 mL) was cooled to −78 °C and treated dropwise over a period of 1 h with a solution of $Cl_2Si_2Me_4$ (126 mg, 0.67 mmol) in pentane (5 mL). After complete addition the reaction mixture was stirred for another 2 h at −78 °C and subsequently allowed to warm to room temperature. During this time the color of the suspension changed from pale brown to deep red and a black precipitate formed. After 12 h all volatiles were removed and the solid was washed with pentane (3×10 mL) and filtered off. The deep red solution was concentrated to about 5 mL and cooled to −70 °C overnight. The red precipitate was washed with cold pentane (3×5 mL, −78 °C) and dissolved in pentane (20 mL) at room temperature. After filtration and removal of the solvent, compound **4** was obtained as a red solid (103 mg, 0.30 mmol, 46 %). Crystals were grown from a saturated pentane solution at −30 °C. ^1H NMR (C_6D_6, 500.1 MHz): $\delta = 0.29$ (s, 12H; $Si(CH_3)_2$), 5.12–5.15 (m, 4H; $CH^{benzene}$), 5.19–5.24 (m, 2H; $CH^{benzene}$), 5.39–5.41 ppm (m, 4H; $CH^{benzene}$); $^{13}C\{^1H\}$ NMR (C_6D_6, 125.8 MHz): $\delta = -2.71$ ($Si(CH_3)_2$), 83.66 ($C^{benzene}H$), 84.40 ($C^{benzene}H$), 85.60 ($C^{benzene}H$), 87.11 ppm ($C^{benzene}$); $^{29}Si\{^1H\}$ NMR (C_6D_6, 99.4 MHz): $\delta = -21.72$; UV/Vis (hexane): λ_{max} (ε) = 239 (11 256), 330 (sh), 375 (18 653), 529 nm (412 L mol^{-1} cm^{-1}); elemental analysis. calcd (%) for $C_{16}H_{22}Si_2Ti$ (318.52): C 60.27, H 7.00; found: C 59.39, H 6.75.

$[Ti(\eta^6\text{-}C_6H_5SntBu_2)_2]$ (5): A slurry of $[Ti(\eta^6\text{-}C_6H_5Li)_2]\cdot pmdta$ (**3**·pmdta) (250 mg, 0.64 mmol) in pentane (10 mL) was cooled to −78 °C and treated dropwise over a period of 1 h with a solution of $Cl_2Sn_2tBu_4$ (362 mg, 0.67 mmol) in pentane (5 mL). After complete addition the reaction mixture was stirred for another 2 h at −78 °C and subsequently allowed to warm to room temperature. During this time the color of the suspension changed from pale brown to deep red and a black precipitate formed. After 12 h all volatiles were removed and the solid was washed with pentane (3×10 mL) and filtered off. The deep red solution was concentrated to about 5 mL and cooled to −70 °C overnight. The red precipitate was washed with cold pentane (3×5 mL, −78 °C) and then dissolved in pentane (20 mL) at room temperature. After filtration and removal of the solvent, compound **5** was obtained as a dark red solid (156 mg, 0.23 mmol, 36 %). Crystals were grown from a saturated pentane solution at −30 °C. ^1H NMR (500.1 MHz, C_6D_6): $\delta = 1.49$ (s, $J(^{119}Sn,^1H_{tBu}) = 66$, $J(^{117}Sn,^1H_{tBu}) = 63$ Hz, 18H; tBu), 5.04–5.08 (m, 2H; $CH^{benzene}$), 5.16–5.20 (m, 4H; $CH^{benzene}$), 5.52–5.54 ppm (m, 4H; $CH^{benzene}$); $^{13}C\{^1H\}$ NMR (125.8 MHz, C_6D_6): $\delta = 32.51$ ($J(^{119}Sn,^{13}C) = 53$, $J(^{117}Sn,^{13}C) = 50$ Hz, $SnC(CH_3)_3$), 33.38 ($J(^{117/119}Sn,^{13}C) = 40$ Hz, $SnC(CH_3)_3$), 81.45 ($C^{benzene}H$), 83.77 ($J(^{117/119}Sn,^{13}C) = 26$ Hz, $C^{benzene}H$), 90.44 ($J(^{117/119}Sn,^{13}C) = 30$ Hz, $C^{benzene}H$), 93.74 ppm ($C^{benzene}$); $^{119}Sn\{^1H\}$ NMR (186.5 MHz, C_6D_6): −31.20 ppm ($J(Sn,^{117/119}Sn) = 1437$ Hz, $J(Sn,^{13}C) = 264$ Hz); UV/Vis (hexane): λ_{max} (ε) = 255 (sh), 325 (sh), 367 (15 011), 522 nm (408 L mol^{-1} cm^{-1}); elemental analysis calcd (%) for $C_{28}H_{46}Sn_2Ti$ (667.95): C 50.35, H 6.94; found: C 49.89, H 6.83.

Synthesis of $[Ti(\eta^6\text{-}C_6H_5)_2SiMe_2]$ (6): A solution of Cl_2SiMe_2 (236 mg, 1.84 mmol) in pentane (10 mL) was added dropwise to a slurry of $[Ti(\eta^6\text{-}C_6H_5Li)_2]\cdot pmdta$ (**3**·pmdta) (598 mg, 1.54 mmol) in pentane (25 mL) at −78 °C over 30 min. After complete addition, the reaction mixture was allowed to warm to room temperature and stirred for 12 h during which the color changed to deep red. All volatiles were removed and the black precipitate was washed with pentane (3×10 mL) and filtered off. The dark red filtrate was reduced to 5 mL, cooled to −70 °C for 24 h, and the orange precipitate washed with cold pentane (3×5 mL) at −78 °C. Compound **6** was obtained as an orange solid after dissolving in pentane, filtration, and removal of all volatiles in vacuum (128 mg, 0.48 mmol, 32 %). ^1H NMR (C_6D_6, 500.1 MHz): $\delta = 0.05$ (s, 6H; $Si(CH_3)_2$), 4.06–4.08 (m, 4H; $CH^{benzene}$), 5.51—5.53 (m, 4H; $CH^{benzene}$), 5.59—5.60 ppm (m, 2H; $CH^{benzene}$); $^{13}C\{^1H\}$ NMR (C_6D_6, 125.8 MHz): $\delta = -8.70$ ($Si(CH_3)_2$), 40.41 ($C^{benzene}$), 73.84 ($C^{benzene}H$), 90.91 ($C^{benzene}H$), 93.81 ppm ($C^{benzene}H$); $^{29}Si\{^1H\}$ NMR (C_6D_6, 99.4 MHz): $\delta = 7.38$; UV/Vis (hexane): λ_{max} (ε) = 245 (sh), 287 (3650), 345 (12 129 L mol^{-1} cm^{-1}), 460 nm (sh); elemental analysis calcd (%) for $C_{14}H_{16}SiTi$ (260.05): C 64.60, H 6.20; found: C 64.13, H 6.20.

Synthesis of $[Ti(\eta^6\text{-}C_6H_5)_2GeMe_2]$ (7): Over a period of 30 min a solution of Cl_2GeMe_2 (170 mg, 0.99 mmol) in pentane (10 mL) was added to a slurry of $[Ti(\eta^6\text{-}C_6H_5Li)_2]\cdot pmdta$ (**3**·pmdta) (320 mg, 0.82 mmol) in pentane (20 mL) at −78 °C. The reaction mixture was allowed to warm to room temperature and was stirred at room temperature over a period of 12 h. All volatiles were removed in vacuum and the black precipitate was washed with pentane (3×10 mL) and filtered off. Concentrating the red solution to approximately 5 mL and storing the mixture at −70 °C overnight gave an orange precipitate, which was washed with cold pentane (3×5 mL), dissolved in warm pentane, and separated from all insoluble material by filtration. The solvent was removed to yield $[Ti(\eta^6\text{-}$

$C_6H_5)_2GeMe_2]$ (**7**) as an orange solid (106 mg, 0.35 mmol, 43 %). Crystals were grown from a saturated pentane solution at room temperature. ^1H NMR (500.1 MHz, C_6D_6): $\delta = 0.15$ (s, 6 H; $Ge(CH_3)_2$), 3.98–4.00 (m, 4 H; $CH^{benzene}$), 5.58–5.59 (m, 2 H; $CH^{benzene}$), 5.61–5.65 ppm (m, 4 H; $CH^{benzene}$); $^{13}C\{^1H\}$ NMR (125.8 MHz, C_6D_6): $\delta = -8.85$ ($Ge(CH_3)_2$), 35.47 ($C^{benzene}$), 75.10 ($C^{benzene}H$), 91.61 ($C^{benzene}H$), 93.70 ppm ($C^{benzene}H$); UV/Vis (hexane): λ_{max} (ε) = 245 (3575), 285 (sh), 348 (12 029), 463 nm (326 $L\,mol^{-1}\,cm^{-1}$); elemental analysis calcd. (%) for $C_{14}H_{16}GeTi$ (304.00): C 55.26, H 5.30; found: C 55.45, H 5.36.

Synthesis of [Ti(η⁶-$C_6H_5)_2$Sn*t*Bu$_2$] (8): A solution of Cl_2Sn*t*Bu$_2$ (553 mg, 1.82 mmol) in pentane (10 mL) was added dropwise to a slurry of $[Ti(\eta^6\text{-}C_6H_5Li)_2]$·pmdta (**3**·pmdta) (530 mg, 1.51 mmol) in pentane (25 mL) at −78 °C over 30 min. After complete addition, the reaction mixture was allowed to warm to ambient temperature over a period of 12 h, during which time the solution color changed to deep red. All volatiles were removed and the black precipitate was washed with pentane (3×10 mL) and filtered off. The dark red filtrate was reduced to 5 mL, cooled to −70 °C for 24 h, and the orange precipitate that formed was washed with cold pentane (3×5 mL) at −78 °C. Compound **8** was obtained as a light red solid after dissolving in pentane again, filtration, and removal of all volatiles in vacuum (190 mg, 0.43 mmol, 29 %). From a saturated pentane solution at −30 °C red crystals suitable for X-ray structure analysis were obtained. ^1H NMR (500.1 MHz, C_6D_6): $\delta = 1.33$ (s, $J(^{119}Sn,^1H_{tBu}) = 71$ Hz, $J(^{117}Sn,^1H_{tBu}) = 68$ Hz, 18 H; $Sn(C(CH_3)_3)$), 4.42–4.45 (m, $J(^{119}Sn,^1H_{tBu}) = 25$ Hz, $J(^{117}Sn,^1H_{tBu}) = 21$ Hz, 4 H; $CH^{benzene}$), 5.52–5.57 (m, 2 H; $CH^{benzene}$), 5.61–5.64 ppm (m, 4 H; $CH^{benzene}$); $^{13}C\{^1H\}$ NMR (125.8 MHz, C_6D_6): $\delta = 32.84$ ($J(^{119}Sn,^{13}C) = 136$ Hz, $J(^{117}Sn,^{13}C) = 99$ Hz, $SnC(CH_3)_3$), 34.19 ($SnC(CH_3)_3$), 46.07 ($C^{benzene}$), 80.47 ($J(^{117/119}Sn,^{13}C) = 18$ Hz, $C^{benzene}H$), 89.96 ($J(^{117/119}Sn,^{13}C) = 9$ Hz, $C^{benzene}H$), 91.40 ppm ($J(^{117/119}Sn,^{13}C) = 30$ Hz, $C^{benzene}H$); $^{119}Sn\{^1H\}$ NMR (186.5 MHz, C_6D_6): $\delta = 2.06$; UV/Vis (hexane): λ_{max} (ε) = 251 (16 258), 290 nm (sh), 350 (14 877), 464 nm (458 $L\,mol^{-1}\,cm^{-1}$); elemental analysis calcd (%) for $C_{20}H_{28}SnTi$ (434.79): C 55.04, H 6.47; found: C 54.47, H 6.35.

X-ray crystallography: The crystal data of compounds **1**, **2**, **4**, **5**, and **8** were collected on a Bruker X8-APEX II diffractometer with a CCD area detector and multi-layer mirror monochromated $Mo_{K\alpha}$ radiation. The crystal data of compound **7** were collected on a Bruker D8-QUEST diffractometer with a CCD area detector and multi-layer mirror monochromated $Mo_{K\alpha}$ radiation. The structures were solved by using direct methods, refined with the Shelx software package and expanded by using Fourier techniques.[26] All non-hydrogen atoms were refined anisotropically. Hydrogen atoms were included in structure factor calculations. All hydrogen atoms were assigned to idealized geometric positions. The crystal of compound **2** was a pseudo-merohedral twin with domains rotated by 179.9° around the real axis [0.199 −0.002 1.000]. The BASF parameter was refined to 29 %. The crystal of compound **1** was a pseudo-merohedral twin with domains rotated by 180.0° around the real axis [−0.175 1.000 −0.010]. The BASF parameter was refined to 40 %. (Figure 6)

*Crystal data for compound **1***: $C_{12}H_{12}Ti$; $M_r = 204.12$; red blocks; $0.22\times0.20\times0.04\ mm^3$; triclinic space group $P\bar{1}$; $a = 6.1005(5)$, $b = 7.8030(6)$, $c = 9.7289(7)$ Å; $\alpha = 88.650(3)$, $\beta = 84.731(3)$, $\gamma = 82.038(3)°$; $V = 456.69(6)$ Å^3; $Z = 2$; $\rho_{calcd} = 1.484\ g\,cm^{-3}$; $\mu = 0.878\ mm^{-1}$; $F(000) = 212$; $T = 100(2)$ K; $R_1 = 0.0242$; $wR^2 = 0.0560$; 1975 independent reflections [$2\theta \le 53.84°$] and 122 parameters.

*Crystal data for compound **2***: $C_{17}H_{20}N_2Ti$; $M_r = 300.25$; black blocks; $0.49\times0.19\times0.10\ mm^3$; monoclinic space group $P2_1/c$; $a = 7.8409(10)$, $b = 22.889(3)$, $c = 7.8881(9)$ Å; $\beta = 101.484(4)°$; $V = 1387.3(3)$ Å^3; $Z = 4$; $\rho_{calcd} = 1.438\ g\,cm^{-3}$; $\mu = 0.608\ mm^{-1}$; $F(000) = 632$; $T = 100(2)$ K; $R_1 = 0.0392$; $wR^2 = 0.0814$; 2740 independent reflections [$2\theta \le 52.04°$] and 184 parameters.

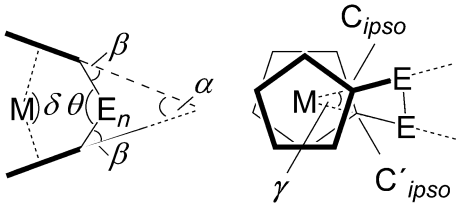

Figure 6. Parameters that define the geometry of *ansa* sandwich compounds on the example of metallocenes (M = central metal, E = bridging element).

*Crystal data for compound **4***: $C_{16}H_{22}Si_2Ti$; $M_r = 318.42$; red block; $0.26\times0.11\times0.04\ mm^3$; orthorhombic space group *Pnma*; $a = 13.2694(6)$, $b = 11.8143(5)$, $c = 9.8493(4)$ Å; $V = 1544.06(11)$ Å^3; $Z = 4$; $\rho_{calcd} = 1.370\ g\,cm^{-3}$; $\mu = 0.694\ mm^{-1}$; $F(000) = 672$; $T = 296(2)$ K; $R_1 = 0.0240$, $wR^2 = 0.0631$; 1730 independent reflections [$2\theta \le 53.52°$] and 99 parameters.

*Crystal data for compound **5***: $C_{28}H_{46}Sn_2Ti$; $M_r = 667.93$; red plates; $0.220\times0.160\times0.065\ mm^3$; monoclinic space group $P2_1/c$; $a = 30.2820(14)$, $b = 11.1978(5)$, $c = 16.8386(8)$ Å; $\beta = 90.586(2)°$; $V = 5709.5(5)$ Å^3; $Z = 8$; $\rho_{calcd} = 1.554\ g\,cm^{-3}$; $\mu = 2.022\ mm^{-1}$; $F(000) = 2688$,; $T = 100(2)$ K; $R_1 = 0.0474$; $wR^2 = 0.0695$; 11 660 independent reflections [$2\theta \le 52.74°$] and 583 parameters.

*Crystal data for compound **7***: $C_{14}H_{16}GeTi$; $M_r = 304.76$; red plates; $0.21\times0.115\times0.05\ mm^3$; monoclinic space group $P2_1/c$; $a = 16.959(6)$, $b = 21.554(8)$, $c = 10.571(4)$ Å; $\beta = 102.766(14)°$; $V = 3769(2)$ Å^3; $Z = 12$; $\rho_{calcd} = 1.611\ g\,cm^{-3}$; $\mu = 2.997\ mm^{-1}$; $F(000) = 1848$; $T = 100(2)$ K; $R_1 = 0.0422$; $wR^2 = 0.0757$; 7693 independent reflections [$2\theta \le 52.746°$] and 439 parameters.

*Crystal data for compound **8***: $C_{20}H_{28}SnTi$; $M_r = 435.01$; red blocks; $0.23\times0.16\times0.15\ mm^3$; monoclinic space group *Cc*; $a = 12.507(16)$, $b = 9.658(13)$, $c = 15.076(19)$ Å; $\beta = 107.49(3)°$; $V = 1737(4)$ Å^3; $Z = 4$; $\rho_{calcd} = 1.663\ g\,cm^{-3}$; $\mu = 1.892\ mm^{-1}$; $F(000) = 880$; $T = 100(2)$ K; $R_1 = 0.0220$; $wR^2 = 0.0450$; 1772 independent reflections [$2\theta \le 52.744°$] and 104 parameters.

Crystallographic data have been deposited with the Cambridge Crystallographic Data Center as supplementary publication no. CCDC 1030722 (**1**), 1047224 (**2**), 1030723 (**4**), 1047225 (**5**), 1030724 (**7**), and 1047226 (**8**). These data can be obtained free of charge from The Cambridge Crystallographic Data Centre via www.ccdc.cam.ac.uk/data_request/cif.

Computational methods: The geometry optimization of compounds **1**, **4**, and **6** without symmetry constraints was carried out at B3LYP[27] by using the basis set of def2-SVP.[28] The structures were characterized as minima by frequency calculations. All calculations were done by using Gaussian 09.[29]

Acknowledgements

Financial support from the Deutsche Forschungsgemeinschaft (DFG) is gratefully acknowledged.

Keywords: arene ligands · Group 14 elements · sandwich complexes · solid-state structures · titanium

[1] a) H. Werner, *Angew. Chem. Int. Ed.* **2012**, *51*, 6052–6058; *Angew. Chem.* **2012**, *124*, 6156–6162; b) T. J. Kealy, P. L. Pauson, *Nature* **1951**, *168*,

1039 – 1040; c) S. A. Miller, J. A. Tebboth, J. F. Tremaine, *J. Chem. Soc.* **1952**, 632 – 635.

[2] E. O. Fischer, W. Hafner, *Z. Naturforsch. Sect. B* **1955**, *10*, 665 – 668.

[3] For the selective 1,1′-dimetalation of $[\mathrm{Fe}(\eta^5\text{-}\mathrm{C_5H_5})_2]$, see: a) M. Walczak, K. Walczak, R. Mink, M. D. Rausch, G. Stucky, *J. Am. Chem. Soc.* **1978**, *100*, 6382 – 6388; b) I. R. Butler, W. R. Cullen, J. Ni, S. J. Rettig, *Organometallics* **1985**, *4*, 2196 – 2201; c) M. D. Rausch, D. J. Ciappenelli, *J. Organomet. Chem.* **1967**, *10*, 127 – 136; for general information about polymers derived from sandwich compounds, see: d) A. S. Abd-El-Aziz, I. Manners, *Frontiers in Transition-Metal-Containing Polymers*, Wiley, New York, **2007**; e) V. Bellas, M. Rehahn, *Angew. Chem. Int. Ed.* **2007**, *46*, 5082 – 5104; *Angew. Chem.* **2007**, *119*, 5174 – 5197; f) Z. Chen, M. D. Foster, W. Zhou, H. Fong, D. H. Reneker, R. Resendes, I. Manners, *Macromolecules* **2001**, *34*, 6156 – 6158; for selected properties of ferrocenyl polymers, see: g) K. H. Pannell, V. I. Imshennik, Y. V. Maksimov, M. N. Il′ina, H. K. Sharma, V. S. Papkov, I. P. Suzdalev, *Chem. Mater.* **2005**, *17*, 1844 – 1850; h) P. W. Cyr, E. J. D. Klem, E. H. Sargent, I. Manners, *Chem. Mater.* **2005**, *17*, 5770 – 5773; i) A. C. Arsenault, V. Kitaev, I. Manners, G. A. Ozin, A. Mihib, H. Míguez, *J. Mater. Chem.* **2005**, *15*, 133 – 138.

[4] a) E. O. Fischer, H. P. Kögler, *Chem. Ber.* **1957**, *90*, 250 – 255; b) D. Seyferth, *Organometallics* **2002**, *21*, 1520 – 1530; c) E. O. Fischer, H.-O. Stahl, *Chem. Ber.* **1956**, *89*, 1805 – 1808; d) H. Braunschweig, T. Kupfer, *Acc. Chem. Res.* **2010**, *43*, 455 – 465; e) D. E. Herbert, U. F. J. Mayer, I. Manners, *Angew. Chem. Int. Ed.* **2007**, *46*, 5060 – 5081; *Angew. Chem.* **2007**, *119*, 5152 – 5173.

[5] For $[\mathrm{V}(\eta^6\text{-}\mathrm{C_6H_6})_2]$, see: a) H. Braunschweig, M. Kaupp, C. J. Adams, T. Kupfer, K. Radacki, S. Schinzel, *J. Am. Chem. Soc.* **2008**, *130*, 11376 – 11393; for $[\mathrm{Cr}(\eta^6\text{-}\mathrm{C_6H_6})_2]$, see: b) C. Elschenbroich, *J. Organomet. Chem.* **1968**, *14*, 157 – 163; for $[\mathrm{Mo}(\eta^6\text{-}\mathrm{C_6H_6})_2]$, see: c) M. L. H. Green, I. Treurnicht, J. A. Bandy, A. Gourdon, K. Prout, *J. Organomet. Chem.* **1986**, *306*, 145 – 165; d) H. Braunschweig, N. Buggisch, U. Englert, M. Homberger, T. Kupfer, D. Leusser, M. Lutz, K. Radacki, *J. Am. Chem. Soc.* **2007**, *129*, 4840 – 4847.

[6] C. Elschenbroich, J. Hurley, B. Metz, W. Massa, G. Baum, *Organometallics* **1990**, *9*, 889 – 897.

[7] a) H. Braunschweig, M. Homberger, C. Hu, X. Zheng, E. Gullo, G. Clentsmith, M. Lutz, *Organometallics* **2004**, *23*, 1968 – 1970; b) H. Braunschweig, C. J. Adams, T. Kupfer, I. Manners, R. M. Richardson, G. R. Whittell, *Angew. Chem. Int. Ed.* **2008**, *47*, 3826 – 3829; *Angew. Chem.* **2008**, *120*, 3886 – 3889; c) C. L. Lund, J. A. Schachner, J. W. Quail, J. Müller, *Organometallics* **2006**, *25*, 5817 – 5823; d) K. C. Hultzsch, J. M. Nelson, A. J. Lough, I. Manners, *Organometallics* **1995**, *14*, 5496 – 5502; e) C. Elschenbroich, E. Schmidt, R. Gondrum, B. Metz, O. Burghaus, W. Massa, S. Wocadlo, *Organometallics* **1997**, *16*, 4589 – 4596; f) H. Braunschweig, T. Kupfer, *Organometallics* **2007**, *26*, 4634 – 4638; g) A. Berenbaum, I. Manners, *Dalton Trans.* **2004**, 2057.

[8] C. L. Lund, J. A. Schachner, J. W. Quail, J. Müller, *J. Am. Chem. Soc.* **2007**, *129*, 9313 – 9320.

[9] a) H. Braunschweig, T. Kupfer, M. Lutz, K. Radacki, F. Seeler, R. Sigritz, *Angew. Chem. Int. Ed.* **2006**, *45*, 8048 – 8051; *Angew. Chem.* **2006**, *118*, 8217 – 8220; b) F. Bauer, H. Braunschweig, K. Schwab, *Organometallics* **2010**, *29*, 934 – 938.

[10] For reduction of $[\mathrm{Ti}(\eta^6\text{-}\mathrm{C_6H_6})_2]$, see: a) J. A. Bandy, A. Berry, M. L. H. Green, R. N. Perutz, K. Prout, J.-N. Verpeauxa, *J. Chem. Soc. Chem. Commun.* **1984**, 729 – 731; for spectroscopic data, see: b) T. D. Jaeger, D. van Heijnsbergen, S. J. Klippenstein, G. von Helden, G. Meijer, M. A. Duncan, *J. Am. Chem. Soc.* **2004**, *126*, 10981 – 10991; c) K. Miyajima, S. Yabushita, M. B. Knickelbein, A. Nakajima, *J. Am. Chem. Soc.* **2007**, *129*, 8473 – 8480; d) B. R. Sohnlein, Y. Lei, D.-S. Yang, *J. Chem. Phys.* **2007**, *127*, 114302; for transition-metal molecular sandwich nanowires, see: e) M. Wu, X. C. Zeng, *Appl. Phys. Lett.* **2011**, *99*, 053121; for titanium benzene multidecker complexes, see: f) Z. Yang, B. Zhang, X. Liu, X. Li, Y. Yang, S. Xionge, B. Xuc, *Phys. Chem. Chem. Phys.* **2014**, *16*, 1902 – 1908; for catalytic reactions with $[\mathrm{Ti}(\eta^6\text{-}\mathrm{C_6H_6})_2]$, see: g) V. M. Akhmedov, M. T. Anthony, M. L. H. Green, D. Young, *J. Chem. Soc. Chem. Commun.* **1974**, 777 – 778; h) C. W. Tullock, F. N. Tebbe, R. Mulhaupt, D. W. Ovenall, R. A. Setterquist, S. D. Ittel, *J. Polym. Sci. Part A* **1989**, *27*, 3063 – 3081; i) E. F. Kvashina, G. N. Petrova, G. P. Belov, O. S. Roshchupkina, O. N. Efimov, *Russ. Chem. Bull.* **2002**, *51*, 817 – 819; j) E. F. Kvashina, Z. M. Dzhabieva, O. N. Efimov, M. G. Kaplunov, *Russ. Chem. Bull.* **2009**, *58*, 1669 – 1671; k) H. Ledon, I. Tkatchenko, D. Young, *Tetrahedron Lett.* **1979**, *20*, 173 – 176.

[11] a) F. W. S. Benfield, M. L. H. Green, J. S. Ogden, D. Young, *J. Chem. Soc. Chem. Commun.* **1973**, 866 – 867; b) F. G. N. Cloke, M. L. H. Green, *J. Chem. Soc. Dalton Trans.* **1981**, 1938 – 1943; c) P. N. Hawker, P. L. Timms, *J. Chem. Soc. Dalton* **1983**, 1123 – 1126.

[12] H. Bönnemann, B. Korall, *Angew. Chem. Int. Ed. Engl.* **1992**, *31*, 1490 – 1492; *Angew. Chem.* **1992**, *104*, 1506 – 1508.

[13] a) G. G. Tairova, E. F. Kvashina, O. N. Krasochka, G. A. Kichigina, Y. A. Shvetsov, E. M. Lisetskii, L. O. Atovmyan, Y. G. Borod′ko, *Nouv. J. Chim.* **1981**, *5*, 603 – 604; b) O. N. Krasochka, A. F. Shestakov, G. G. Tairova, Y. A. Shvetsov, E. F. Kvashina, V. I. Ponomarev, L. O. Atovmyan, Y. G. Borod′ko, *Khim. Fiz.* **1983**, *11*, 1459 – 1467.

[14] a) G. G. Tairova, O. N. Krasochka, V. I. Ponomaryov, E. F. Kvashina, Y. A. Shvetsov, E. M. Lisetsky, D. P. Kiryukhin, L. O. Atovmyan, Y. G. Borod′ko, *Trans. Metal Chem.* **1982**, *7*, 189 – 190; b) D. W. Blackburn, D. Britton, J. E. Ellis, *Angew. Chem. Int. Ed. Engl.* **1992**, *31*, 1495 – 1498; *Angew. Chem.* **1992**, *104*, 1520 – 1523.

[15] a) M. Tamm, A. Kunst, T. Bannenberg, E. Herdtweck, P. Sirsch, C. J. Elsevier, J. M. Ernsting, *Angew. Chem. Int. Ed.* **2004**, *43*, 5530 – 5534; *Angew. Chem.* **2004**, *116*, 5646 – 5650; b) M. Tamm, A. Kunst, T. Bannenberg, E. Herdtweck, R. Schmid, *Organometallics* **2005**, *24*, 3163 – 3171; c) R. J. Baker, T. Bannenberg, A. Kunst, S. Randoll, M. Tamm, *Inorg. Chim. Acta* **2006**, *359*, 4797 – 4801; d) M. Tamm, A. Kunst, T. Bannenberg, A. Randoll, P. G. Jones, *Organometallics* **2007**, *26*, 417 – 424; e) M. Tamm, *Chem. Commun.* **2008**, 3089 – 3100; f) S. Büschel, T. Bannenberg, C. G. Hrib, A. Glöckner, P. G. Jones, M. Tamm, *J. Organomet. Chem.* **2009**, *694*, 1244 – 1250.

[16] A. J. Arduengo, H. V. Rasika Dias, R. L. Harlow, M. Kline, *J. Am. Chem. Soc.* **1992**, *114*, 5530 – 5534.

[17] N. Kuhn, T. Kratz, D. Bläser, R. Boese, *Inorg. Chim. Acta* **1995**, *238*, 179 – 181.

[18] a) A. G. Osborne, R. H. Whiteley, *J. Organomet. Chem.* **1975**, *101*, C27 – C28; b) A. G. Osborne, R. H. Whiteley, *J. Organomet. Chem.* **1980**, *193*, 345 – 357; c) R. Rulkens, A. J. Lough, I. Manners, *Angew. Chem. Int. Ed. Engl.* **1996**, *35*, 1805 – 1807; *Angew. Chem.* **1996**, *108*, 1929 – 1931.

[19] a) H. Braunschweig, M. Fuß, S. K. Mohapatra, K. Kraft, T. Kupfer, M. Lang, K. Radacki, C. G. Daniliuc, P. G. Jones, M. Tamm, *Chem. Eur. J.* **2010**, *16*, 11732 – 11743; b) A. C. Tagne Kuate, C. G. Daniliuc, P. G. Jones, M. Tamm, *Eur. J. Inorg. Chem.* **2012**, 1727.

[20] B. Cordero, V. Gómez, A. E. Platero-Prats, M. Revés, J. Echeverría, E. Cremades, F. Barragán, S. Alvarez, *Dalton Trans.* **2008**, 2832.

[21] H. Braunschweig, A. Damme, K. Dück, T. Kramer, I. Krummenacher, K. Radacki, S. Stellwag-Konertz, *J. Am. Chem. Soc.* **2015**, *137*, 1492 – 1500.

[22] H. Braunschweig, F. Breher, S. Capper, K. Dück, M. Fuß, J. O. C. Jimenez-Halla, I. Krummenacher, T. Kupfer, D. Nied, K. Radacki, *Chem. Eur. J.* **2013**, *19*, 270 – 281.

[23] T. Schaub, M. Backes, U. Radius, *Organometallics* **2006**, *25*, 4196 – 4206.

[24] U. Englich, U. Hermann, I. Prass, T. Schollmeier, K. Ruhlandt-Senge, F. Uhlig, *J. Organomet. Chem.* **2002**, *646*, 271 – 276.

[25] C. A. Brown, S. Krishnamurthy, *J. Organomet. Chem.* **1978**, *156*, 111.

[26] G. Sheldrick, *Acta Crystallogr. Sect. A* **2008**, *64*, 112 – 122.

[27] a) A. D. Becke, *J. Chem. Phys.* **1993**, *98*, 5648; b) A. D. Becke, *Phys. Rev. A* **1988**, *38*, 3098; c) C. Lee, W. Yang, W. G. Parr, *Phys. Rev. B* **1988**, *37*, 785.

[28] A. Schäfer, H. Horn, R. Ahlrichs, *J. Chem. Phys.* **1992**, *97*, 2571.

[29] Gaussian 09, Revision D.01, M. J. Frisch, G. W. Trucks, H. B. Schlegel, G. E. Scuseria, M. A. Robb, J. R. Cheeseman, G. Scalmani, V. Barone, B. Mennucci, G. A. Petersson, H. Nakatsuji, M. Caricato, X. Li, H. P. Hratchian, A. F. Izmaylov, J. Bloino, G. Zheng, J. L. Sonnenberg, M. Hada, M. Ehara, K. Toyota, R. Fukuda, J. Hasegawa, M. Ishida, T. Nakajima, Y. Honda, O. Kitao, H. Nakai, T. Vreven, J. A. Montgomery, Jr., J. E. Peralta, F. Ogliaro, M. Bearpark, J. J. Heyd, E. Brothers, K. N. Kudin, V. N. Staroverov, R. Kobayashi, J. Normand, K. Raghavachari, A. Rendell, J. C. Burant, S. S. Iyengar, J. Tomasi, M. Cossi, N. Rega, N. J. Millam, M. Klene, J. E. Knox, J. B. Cross, V. Bakken, C. Adamo, J. Jaramillo, R. Gomperts, R. E. Stratmann, O. Yazyev, A. J. Austin, R. Cammi, C. Pomelli, J. W. Ochterski, R. L. Martin, K. Morokuma, V. G. Zakrzewski, G. A. Voth, P. Salvador, J. J. Dannenberg, S. Dapprich, A. D. Daniels, Ö. Farkas, J. B. Foresman, J. V. Ortiz, J. Cioslowski, D. J. Fox, Gaussian, Inc., Wallingford CT, **2009**.

Received: February 23, 2015